International Core Journal of Engineering Volume 8 Issue 8, 2022
ISSN: 2414-1895 DOI: 10.6919/ICJE.202208_8(8).0050

Basic and Crucial Calculations of Coordinate System Establishments and Digital Model Operations for Dental 3D Printing

Zhihui Pan[1], Hongwei Wang[2], Xueqian Chen[2], Qiming Chen[3], and Jinyun Zhou[1,*]

[1] School of Physics and Optoelectronic Engineering, Guangdong University of Technology, Guangzhou 510006, China

[2] Guangzhou Riton Biomaterial Co., Ltd, Guangzhou 510038, China

[3] School of Mechanical and Electrical Engineering, Guangdong Polytechnic of Industry and Commerce, Guangzhou, 510510, China

Abstract

Objectives: Different kinds of coordinate systems were calculated and established to quantitatively describe spatial operations in digital dentistry to solve the problem of few relevant reports from underlying mathematical calculation to top-level software design so far. Methods: The absolute coordinate system (A-CS) of the whole teeth was calculated by three easily available feature points to determine views of models. The relative coordinate system (R-CS) of a single tooth with automatically generated coordinate axes was used the oriented bounding box (OBB) method based on principal component analysis (PCA) to determine. The default coordinate system (D-CS) is generated by the using software. Results: It is the R-CS that remains relative positions and relationships of a single tooth unchanged in operation, which makes independent analysis into reality. The combination of A-CS and R-CS judges every tooth and reversely calculates operations, which realizes independent operations and simple calculations of globalizations and localizations. The transformation matrix based on axis-angle realized the simultaneous rotation and translation, calculating the mutual transformations in different positions and coordinate systems. Conclusions: The digital calculations and operations in different coordinate systems demonstrated the good performance for transformations between local and whole models. Clinical significance: The calculations of appropriate coordinate systems are basic and essential for complete digital operations in dental treatments and 3D printing.

Keywords

Digital Models; Mathematical Calculations; Coordinate Systems; Axis-angle; Matrix; 3D Printing.

1. Introduction

More and more attention has been paid to dental fields for many reasons, such as economic impact [1], oral diseases [2], oral health [3] and people's pursuit of beauty [4-6]. With the development of computer-aided design (CAD) and computer-aid manufacturing (CAM), the digital models have been widely used in many areas for many advantages including instant accessibility of 3D information [7], the smaller error [8], the visualization [9], as well as accuracy and reliability [10]. Consequently, many new three-dimensional (3D) data acquirement technologies [11, 12] have been explored to achieve extracting and processing digital models. Intraoral scanners are commonly used to scan and

ISSN: 2414-1895 DOI: 10.6919/ICJE.202208_8(8).0050

extract dentitions to generate accurate 3D digital tooth models [13-15]. The format of stereolithography (STL) [16] is one of the optimum methods to transfer the 3D models to 3D digital information and has been standard for data input of all types of rapid prototyping systems [17], which advocates the evolution of virtual dental fields.

Traditionally, processing teeth was always handled by professionals to generate personal treatments and devices, the speed and quality of teeth processing were based on the experience of the operators, and the next operation must be determined by the result of the previous step in the phased multi-step practice. This has greatly limited the development and breakthrough of relevant fields for the reasons that full manual operations cannot provide predictable results and consume a lot of time and energy. Compared with the traditional methods, the advantages of digital models in orthodontic consist of no real space for storage, easier acquirement and measurement, least chance of failure or breakage [18], and the convenience of recording and sharing of data [19-21]. When dealing with the digital teeth models, data are acquired from the information of triangular meshes. And it is beneficial for automatically manipulating the dental data to make full use of the advantages of mathematical calculations to generate some algorithms. The combination of mathematical calculations and computer-aided technology accelerates and facilitates processing digital models with lower cost and better stage visualization.

The finite helical axis system and the rectangular coordinate system are used to perform biomechanical analyses [22]. Besides, the calculation for convenient operations is also needed to be considered. It is very important to establish proper coordinate systems and views to correctly align medical images with viewers' positions [23, 24]. Though various methods have been taken to process teeth models, the specific and proper mathematical realization of the teeth models in virtual environments has not been studied carefully.

The method of principal component analysis (PCA) is widely used in calculations to find the directions of the largest variance from a numerical data set [25-27]. Though the oriented bounding box (OBB) [28] is always used in collision detection for teeth [29, 30], it can generate three vertical directions, which can be coordinate axes of rectangular coordinate system.

The aim of the coordinate calculation was to better understand and operate the digital models in dentistry.

2. Materials and Methods

2.1 Data Acquisition

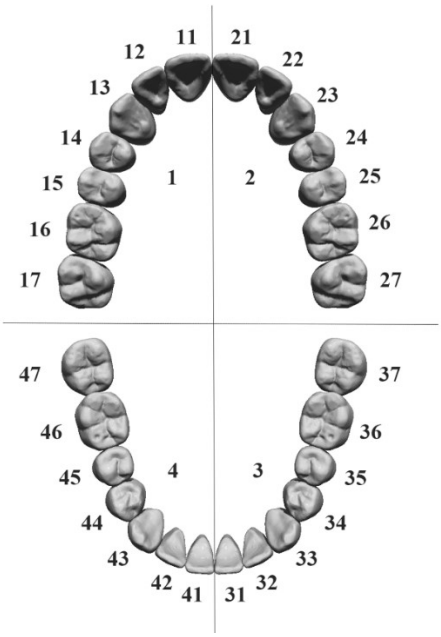

Figure 1. FDI two-digit tooth position representation of 3D digital models.

ISSN: 2414-1895 DOI: 10.6919/ICJE.202208_8(8).0050

All 3D surface dental models were extracted and obtained by intraoral scanners (3Shape) in the Guangzhou company called eBrace. The teeth were numbered by using the method of two-digit dental position recording in Federation Dentaire International (FDI) system [31] (Figure 1).

2.2 Mathematical Method

Three feature points were easily selected on the dental model and the center of these points was chosen as the origin of the A-CS for convenient and simple operations. The directions of the coordinate axes were calculated by the relationships of the vectors. The positive directions of the coordinate axes were selected on the basis of the practical operation habit. The A-CS of the dental model was established by the rule of right-handed Cartesian coordinate system.

To find the origin of R-CS quickly and easily, the mean coordinate value of all sample points on a single tooth was calculated. The OBB method based PCA was taken to generate the directions of three coordinate axes. The positive directions of the coordinate axes were chosen by the practical operation habit and the R-CS of a single tooth was established by the rule of the Cartesian right-handed coordinate system. The R-CS established by OBB method based on PCA will not change even with the shift of location and angle. It is extremely suitable to establish the relative coordinate system for a single tooth.

In most cases, the system automatically will establish the D-CS after the 3D model is imported into the software, and all operations are based on coordinates in this coordinate system. But the coordinate system is always not what we want to process the dental models in. The establishment of proper systems is very important. The relationships of different systems were calculated to reset the coordinate systems and unify the D-CS, A-CS and R-CS.

Normally, the matrices and the vectors are always used to calculate rotations and translations respectively. However, the transformation matrix can make rotate and translate simultaneously. And the coordinates in other coordinate systems are calculated when the coordinates in one coordinate system are known by the transformation matrices. The transformation matrix provides a possible way to express the relationships and reset the coordinate systems.

3. Results and Discussion

3.1 A-CS for Whole Teeth

To facilitate the operations, the mesial adjacent points of the two central incisors (number 31 and 41, set as $\boldsymbol{A}(a_1, a_2, a_3)$) and the distal buccal apex of the bilateral first molars (number 46 and 36, set as $\boldsymbol{B}(b_1, b_2, b_3)$ and $\boldsymbol{C}$) of the lower jaw were easily selected to form a plane (Figure 2(a)). The midpoint of the three points was selected as the coordinate origin $\boldsymbol{O}(0,0,0)$ to establish the A-CS of the whole teeth. The vector direction from the origin O to the mesial adjacent point of the two mandibular central incisors (number 31 and 41) was set as the positive direction of the $\boldsymbol{Y}$-axis. The normal vector of the plane was calculated as $\boldsymbol{Z}$-axis direction by vector product, and the direction from the midpoint to maxilla was defined as the positive direction of the $\boldsymbol{Z}$-axis. The vector product was used to calculate the positive $\boldsymbol{X}$-axis direction by using the positive direction of the $\boldsymbol{Y}$-axis and $\boldsymbol{Z}$-axis. In the whole teeth model, the positive direction of the $\boldsymbol{X}$-axis was from the midpoint to the labial side. The axes of $\boldsymbol{X}, \boldsymbol{Y}$ and $\boldsymbol{Z}$ were established an A-CS by the rules of the right-handed Cartesian coordinate system. The unit positive direction vectors $\boldsymbol{i}, \boldsymbol{j}, \boldsymbol{k}$ of $\boldsymbol{X}, \boldsymbol{Y}, \boldsymbol{Z}$ were calculated by the following equations.

ISSN: 2414-1895 DOI: 10.6919/ICJE.202208_8(8).0050

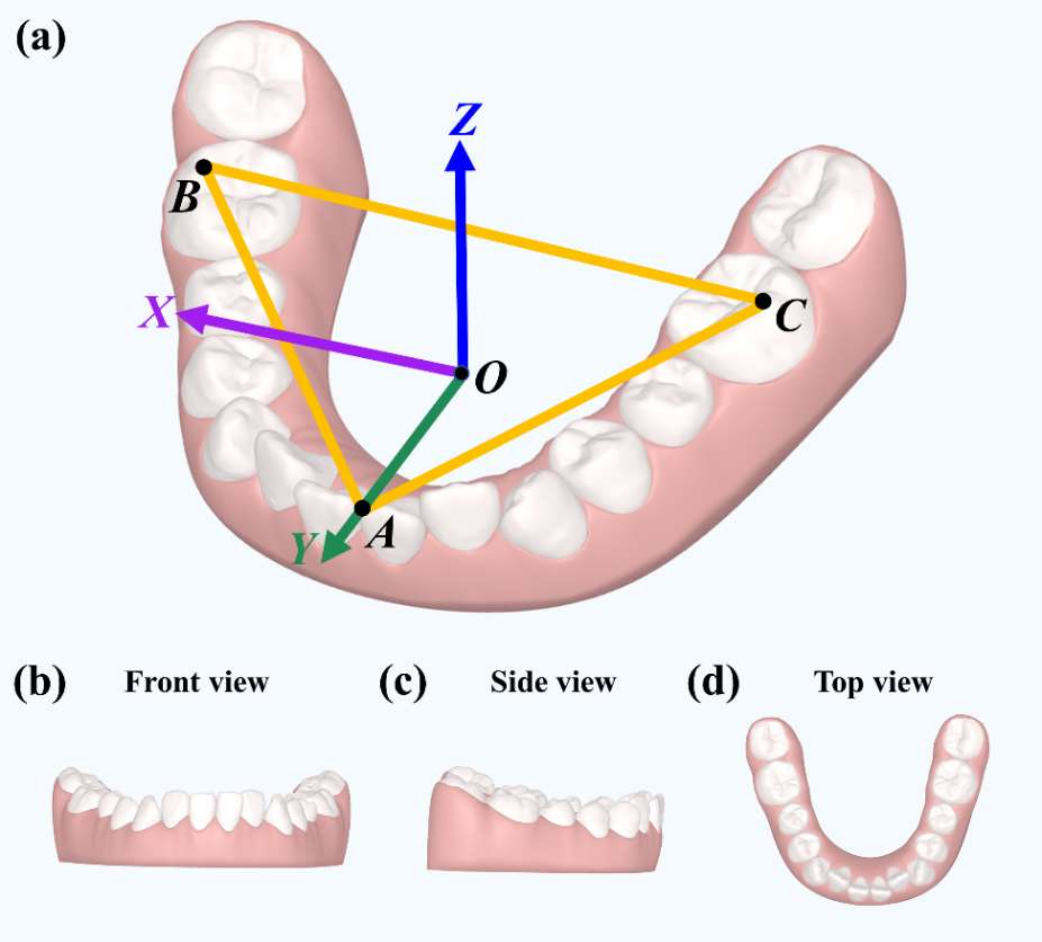

Figure 2. Diagram of the A-CS and the three-view drawing of the whole teeth model. (a) The original point and coordinate axes were ensured by three easily chosen feature points of the model. A three-view drawing of the whole teeth model including (b) front view, (c) side view and (d) top view.

$$\boldsymbol{j} = \frac{\overrightarrow{OA}}{|\overrightarrow{OA}|} = \frac{\begin{bmatrix} a_1 \\ a_2 \\ a_3 \end{bmatrix}}{\sqrt{{a_1}^2+{a_2}^2+{a_3}^2}} \tag{1}$$

$$\mathbf{k} = \frac{\overrightarrow{OB}\times\overrightarrow{OA}}{|\overrightarrow{OB}\times\overrightarrow{OA}|} = \frac{\begin{bmatrix} a_3b_2-a_2b_3 \\ a_1b_3-a_3b_1 \\ a_2b_1-a_1b_2 \end{bmatrix}}{\sqrt{(a_3b_2-a_2b_3)^2+(a_1b_3-a_3b_1)^2+(a_2b_1-a_1b_2)^2}} \tag{2}$$

$$\boldsymbol{i} = \boldsymbol{j}\times\boldsymbol{k} = \frac{\begin{bmatrix} a_2(a_2b_1-a_1b_2)-a_3(a_1b_3-a_3b_1) \\ a_3(a_3b_2-a_2b_3)-a_1(a_2b_1-a_1b_2) \\ a_1(a_1b_3-a_3b_1)-a_2(a_3b_2-a_2b_3) \end{bmatrix}}{\sqrt{{a_1}^2+{a_2}^2+{a_3}^2}\sqrt{(a_3b_2-a_2b_3)^2+(a_1b_3-a_3b_1)^2+(a_2b_1-a_1b_2)^2}} \tag{3}$$

The A-CS of the whole teeth model, played an important role in 3D digital models processing, was used as a reference system of every single tooth. As a consequence, the character of the A-CS remained unchanged in every tooth processing was equal to the world coordinate system in the whole teeth model. Furthermore, the A-CS determined the three-view drawing of the teeth model to facilitate the observations in all directions. The perspective facing the positive direction of Y-axis was the front view (Figure 2(b)), X-axis was the side view (Figure 2(c)), and Z-axis was the top view (Figure 2(d)).

ISSN: 2414-1895 DOI: 10.6919/ICJE.202208_8(8).0050

If operators needed to observe the model on both sides, it met the requirement by viewing models facing both the positive and negative directions of the coordinate axis respectively. For operators, three-view was used to provide the convenient observation of the overall situation of the whole 3D teeth model.

3.2 R-CS for Single Tooth

To ensure independent operations of a single tooth, we calculated and established the R-CS for every tooth by the method of OBB based on the PCA. In the coordinate system, the n points on the digital triangular mesh of a single tooth were chosen to find the most suitable orientations of the tooth. The covariances of the data points were calculated by Equation (4) to form the covariance matrix $\mathbf{H}$ (Equation (5)) to judge the degree of linear correlation between the three dimensions. The equation $cov(\boldsymbol{X},\boldsymbol{Y}) = cov(\boldsymbol{Y},\boldsymbol{X})$ indicates that the covariance matrix is a real symmetric matrix. According to the equation $cov(\boldsymbol{X},\boldsymbol{X}) = D(\boldsymbol{X})$, the principal diagonal elements of $\mathbf{H}$ were the variances of the sample points in different dimensions. The larger the off-diagonal element value of $\mathbf{H}$ is, the greater the correlation degree of the sample points is. The directions of the OBB of a single tooth are highly relevant to the main components of the covariance matrix. As a result, the main diagonal elements of the covariance matrix are required to be larger, while the other elements are desired to be smaller. Using the similar diagonalization of the covariance matrix $\mathbf{H}$ to reduce all the off-diagonal elements to zero. The orthogonal matrix $\mathbf{Q}$ existed in that $\mathbf{H}$ was a real symmetric matrix. The eigenvalues of matrix $\mathbf{H}$ sorted from large to small formed the diagonal matrix $\mathbf{\Lambda}$ and the eigenvectors corresponding to the eigenvalues formed the rows of the orthogonal matrix $\mathbf{Q}$. Then the relationship $\mathbf{H} = \mathbf{Q\Lambda Q^T}$of $\mathbf{H}$ and $\mathbf{Q}$ was calculated by the diagonal matrix $\mathbf{\Lambda}$ after similar diagonalization. And each row of the orthogonal matrix $\mathbf{Q}$ was utilized as an optimal direction of the OBB. The three vectors formed the three coordinate-axis-direction vectors of the R-CS of a single tooth. The unit axis vectors $\boldsymbol{e_1}, \boldsymbol{e_2}, \boldsymbol{e_3}$ of R-CS were obtained by unitization. Equation (6) was used to respectively calculate projections $\mathrm{Pro_{ij}}$ of each $\boldsymbol{P_i}(x_i, y_i, z_i)$ $(i = 1,2,\cdots n)$ of n points in the three unit-axis vectors $\boldsymbol{e_j}$ $(j = 1, 2, 3)$. The length of the projection is either positive or negative, indicating that the projection is in the positive or negative direction of the coordinate axis. Equation (7) was used to calculate the average values of the three components of all sample points of a single tooth, so the central point in OBB of a single tooth was obtained as the origin o of the R-CS.

$$\mathrm{cov}(\boldsymbol{X},\boldsymbol{Y}) = \mathrm{E}[\boldsymbol{X} - \mathrm{E}(\boldsymbol{X})][\boldsymbol{Y} - \mathrm{E}(\boldsymbol{Y})] = \mathrm{E}(\boldsymbol{XY}) - \mathbf{E}(\boldsymbol{X})\mathbf{E}(\boldsymbol{Y}) \tag{4}$$

$$\mathbf{H} = \begin{bmatrix} \mathrm{cov}(\mathbf{X},\mathbf{X}) & \mathrm{cov}(\mathbf{X},\mathbf{Y}) & \mathrm{cov}(\mathbf{X},\mathbf{Z}) \\ \mathrm{cov}(\mathbf{Y},\mathbf{X}) & \mathrm{cov}(\mathbf{Y},\mathbf{Y}) & \mathrm{cov}(\mathbf{Y},\mathbf{Z}) \\ \mathrm{cov}(\mathbf{Z},\mathbf{X}) & \mathrm{cov}(\mathbf{Z},\mathbf{Y}) & \mathrm{cov}(\mathbf{Z},\mathbf{Z}) \end{bmatrix} \tag{5}$$

$$Pro_{ij} = |\boldsymbol{OP_i}| \cos\beta_{ij} = \boldsymbol{OP_i} \cdot \boldsymbol{e_j} \qquad (i = 1,2,\cdots n;\ j = 1,2,3) \tag{6}$$

$$o = \left(\frac{\sum_{i=1}^{n} x_i}{n}, \frac{\sum_{i=1}^{n} y_i}{n}, \frac{\sum_{i=1}^{n} z_i}{n}\right)\ (i = 1,2,\cdots n) \tag{7}$$

Three coordinate axes $\boldsymbol{e_1}, \boldsymbol{e_2}, \boldsymbol{e_3}$ and the origin o were used to establish the R-CS of a single tooth on the basis of right-handed Cartesian coordinate system rules. Figure 3 shows the R-CSs of different teeth of the lower jaw model in the 3D triangular digital grid. The establishment of R-CS suggests that every single tooth in the whole teeth model could be operated independently, which effectively avoided the interferences of other parts of the model excluding the chosen tooth.

ISSN: 2414-1895 DOI: 10.6919/ICJE.202208_8(8).0050

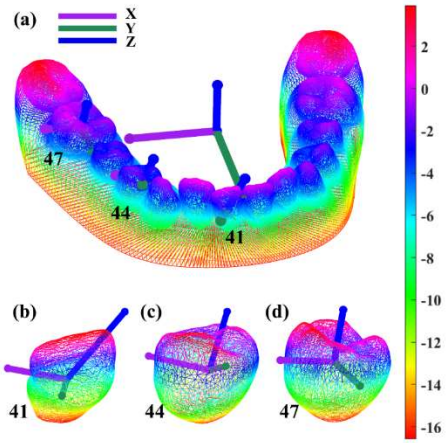

Figure 3. The R-CS of different teeth of the lower jaw model in the 3D triangular digital grid. The purple axis is the X-axis, the green axis is Y-axis and the blue axis is Z-axis of the coordinate system. The right color code shows the Z-axis projection of the position in the model. (a) The A-CS of the whole model and the R-CSs in different teeth consist of tooth positions: (b) 46, (c) 44 and (d) 41.

Once a selected tooth was rotated, the coordinate of every point on the digital tooth changed in the world coordinate system. However, the relative position of each point was unchanged relative to the tooth itself. This made it very complicated to explore the geometric motions of the teeth in a single-step operation. Especially in the process of multiple operations on a single tooth, it became very difficult to analyze the correspondences between the step-by-step operation and the final comprehensive operations. It was essentially an irreconcilable contradiction between the coordinate always changed in the multi-step model operations and the expectation of unchanged relative relationships in the divided manipulation in the world system. Therefore, it was eager to have an intuitive quantity to better reflect the relative positional relationship of each point in a single tooth model. In the R-CS, both the location and the coordinate of a selected point remain the same during rotations and translations.

Since the relative relationship between the R-CS and the single tooth kept unchanged whatever rotations and translations took place in the single tooth, the OBB method based on the PCA was selected to establish the R-CS. Then the rotations and the translations of a single tooth were operated in the coordinate system.

3.3 Transformation between A-CS of the Whole Teeth and R-CS of a Single Tooth

To realize the mutual conversion between systems, Equation (8) was used to calculate the conversion between the A-CS of the whole teeth and the R-CS of a single tooth in the software D-CS. $[X_1 \quad Y_1 \quad Z_1]^T$ was the coordinate of a certain point $\boldsymbol{P}$ in the coordinate system Ω_1. $[X_2 \quad Y_2 \quad Z_2]^T$ referred to the coordinate of point $\boldsymbol{P}$ in the coordinate system Ω_2. The transformation matrix of rotation and translation from the coordinate system Ω_1 to the coordinate system Ω_2 was $[\mathbf{R} \quad \boldsymbol{T}]$, where $\mathbf{R}$ was the unit orthogonal rotation matrix described the rotation relationship between the two coordinate systems and $\boldsymbol{T}$ was the translation matrix described the position translation relationship between the two coordinate systems. The Equation (8) shows a matrix with three rows and 4 columns to finish the transformation among different systems.

$$\begin{bmatrix} X_2 \\ Y_2 \\ Z_2 \end{bmatrix} = [\mathbf{R} \quad \boldsymbol{T}] \begin{bmatrix} X_1 \\ Y_1 \\ Z_1 \\ 1 \end{bmatrix} = \begin{bmatrix} r_{11} & r_{12} & r_{13} & t_X \\ r_{21} & r_{22} & r_{23} & t_Y \\ r_{31} & r_{32} & r_{33} & t_Z \end{bmatrix} \begin{bmatrix} X_1 \\ Y_1 \\ Z_1 \\ 1 \end{bmatrix} \tag{8}$$

ISSN: 2414-1895 DOI: 10.6919/ICJE.202208_8(8).0050

To calculate the rotation matrix R between the two coordinate systems, the method of axis-angle was used to convert the axis and angle into a matrix. Owing to the reason that the other two axes would rotate synchronously when the rotation took place around one axis, the rotation was only calculated once in the Cartesian coordinate system. The unit rotation axis $\boldsymbol{Axis}$ was calculated by Equation (9) with rotation from the unit vector $\boldsymbol{N_{1Z}} = [\mathrm{X_{1Z}} \quad \mathrm{Y_{1Z}} \quad \mathrm{Z_{1Z}}]^T$ of the Z-axis on the coordinate system Ω_1 to the unit vector $\boldsymbol{N_{2Z}} = [\mathrm{X_{2Z}} \quad \mathrm{Y_{2Z}} \quad \mathrm{Z_{2Z}}]^T$ of the Z-axis on the coordinate system Ω_2.

$$\boldsymbol{Axis} = \frac{\boldsymbol{N_{1Z}} \times \boldsymbol{N_{2Z}}}{|\boldsymbol{N_{1Z}} \times \boldsymbol{N_{2Z}}|} = \frac{[\mathrm{Y_{1Z}Z_{2Z} - Y_{2Z}Z_{1Z}} \quad \mathrm{X_{2Z}Z_{1Z} - X_{1Z}Z_{2Z}} \quad \mathrm{X_{1Z}Y_{2Z} - X_{2Z}Y_{1Z}}]^T}{\sqrt{(\mathrm{Y_{1Z}Z_{2Z} - Y_{2Z}Z_{1Z}})^2 + (\mathrm{X_{2Z}Z_{1Z} - X_{1Z}Z_{2Z}})^2 + (\mathrm{X_{1Z}Y_{2Z} - X_{2Z}Y_{1Z}})^2}} \tag{9}$$

The rotation angle θ rotated counterclockwise around the axis between two coordinate systems, and it was calculated by Equation (10).

$$\theta = \cos^{-1} \frac{\boldsymbol{N_{1Z}} \cdot \boldsymbol{N_{2Z}}}{|\boldsymbol{N_{1Z}}||\boldsymbol{N_{2Z}}|} = \cos^{-1} \frac{\mathrm{X_{1Z}X_{2Z} + Y_{1Z}\,Y_{2Z} + Z_{1Z}Z_{2Z}}}{\sqrt{\mathrm{X_{1Z}}^2 + \mathrm{Y_{1Z}}^2 + \mathrm{Z_{1Z}}^2}\sqrt{\mathrm{X_{2Z}}^2 + \mathrm{Y_{2Z}}^2 + \mathrm{Z_{2Z}}^2}} \tag{10}$$

The rotation matrix R from the coordinate system Ω_1 to the coordinate system Ω_2 was calculated by Equation (11), where the three components of $\boldsymbol{Axis}$ were recorded as $\mathrm{X_Z}, \mathrm{Y_Z}, \mathrm{Z_Z}$.

$$\mathbf{R} = \begin{bmatrix} (1-\cos\theta)\mathrm{X_Z}^2 + \cos\theta & (1-\cos\theta)\mathrm{X_Z Y_Z} - \mathrm{Z_Z}\sin\theta & (1-\cos\theta)\mathrm{X_Z Z_Z} + \mathrm{Y_Z}\sin\theta \\ (1-\cos\theta)\mathrm{X_Z Y_Z} + \mathrm{Z_Z}\sin\theta & (1-\cos\theta)\mathrm{Y_Z}^2 + \cos\theta & (1-\cos\theta)\,\mathrm{Y_Z Z_Z} - \mathrm{X_Z}\sin\theta \\ (1-\cos\theta)\mathrm{X_Z Z_Z} - \mathrm{Y_Z}\sin\theta & (1-\cos\theta)\mathrm{Y_Z Z_Z} + \mathrm{X_Z}\sin\theta & (1-\cos\theta)\mathrm{Z_Z}^2 + \cos\theta \end{bmatrix} \tag{11}$$

When the positions in a software system did not overlap before and after model segmentation, the D-CS in the software of the whole dental model was Ω_D with the origin coordinate $\boldsymbol{O_D}(0,0,0)$, and the D-CS of a single tooth operated independently in software was $\Omega_D{}'$ with different origin coordinate $\boldsymbol{O_D}'(\mathrm{X_{O_D}}', \mathrm{Y_{O_D}}', \mathrm{Z_{O_D}}')$ (see Figure 4). Set Ω_A and $\boldsymbol{O_A}(\mathrm{X_A}, \mathrm{Y_A}, \mathrm{Z_A})$ as the A-CS and original coordinate of the whole teeth. Similarly, Ω_R and $O_R(\mathrm{X_R}, \mathrm{Y_R}, \mathrm{Z_R})$ represents the R-CS and original coordinate of a single tooth. The translation matrix is $\boldsymbol{T_{O_A O_R}} = [\mathrm{X_R - X_A} \quad \mathrm{Y_R - Y_A} \quad \mathrm{Z_R - Z_A}]^{\mathrm{T}}$. After the unit rotation axis and rotation angle are calculated in Equation $(9, 10)$, the transformation matrix between the A-CS and R-CS can be calculated by Equation $(8, 11)$.

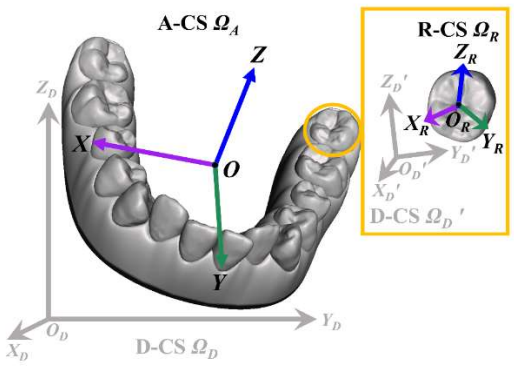

Figure 4. The diagram of all possible coordinate systems in 3D digital processing software including the automatically generated D-CS by models importing in software, the A-CS of the whole teeth and the R-CS of a single tooth in the 3D dental model.

ISSN: 2414-1895 DOI: 10.6919/ICJE.202208_8(8).0050

3.4 The Transformation Matrix

The two D-CSs in the whole model and the single tooth can coincide in a few 3D dental software on the market with $\Omega_D = \Omega_D{}'$. The translation vector is $\boldsymbol{T}_{\boldsymbol{O_D{}'O_D}} = [0 \quad 0 \quad 0]^T$ in this situation, the transformation matrix $[\mathbf{R} \quad \boldsymbol{T}]$ based on rotation and translation is simplified to $\mathbf{R}$. However, to realize the independent operation of a single tooth, the conversion relationship must be calculated for the synchronous operation for the two non-overlapping D-CSs in many software. The translation vector from the coordinate system $\Omega_D{}'$ to the coordinate system Ω_D is $\boldsymbol{T}_{\boldsymbol{O_DO_D{}'}} = [\mathrm{X}_{\mathrm{O_D}'} \quad \mathrm{Y}_{\mathrm{O_D}'} \quad \mathrm{Z}_{\mathrm{O_D}'}]^{\mathrm{T}}$. To calculate rotation or coincide the two coordinate systems, the easiest way is to select the unit vector of a certain axis in two coordinate systems. Then the unit rotation axis is expressed by $\boldsymbol{Axis} = \frac{[-\mathrm{Y}_{\mathrm{D}'} \quad \mathrm{X}_{\mathrm{D}'} \quad 0]^{\mathrm{T}}}{\sqrt{\mathrm{Y}_{\mathrm{D}'}{}^2+\mathrm{X}_{\mathrm{D}'}{}^2}}$, where $\boldsymbol{Z}_{\boldsymbol{O_D}} = [0 \quad 0 \quad 1]^{\mathrm{T}}$ is the unit vector in Z-axis of coordinate system and $\boldsymbol{N}_{\boldsymbol{O_D}'} = [\mathrm{X}_{\mathrm{D}'} \quad \mathrm{Y}_{\mathrm{D}'} \quad \mathrm{Z}_{\mathrm{D}'}]^{\mathrm{T}}$ is the unit vector in $\boldsymbol{Z}$-axis of the coordinate system $\Omega_D{}'$. Simultaneously, the rotation angle $\theta = \cos^{-1}\mathrm{Z}_{\mathrm{D}'}$ is calculated. The components of $\boldsymbol{Axis}$ are set as $\mathrm{X}_{\mathrm{Z}}, \mathrm{Y}_{\mathrm{Z}}, \mathrm{Z}_{\mathrm{Z}}$. Equation (12) calculates the transformation relationship by transformation matrix of any point P between the coordinate $[\mathrm{X}_{1\mathrm{P}} \quad \mathrm{Y}_{1\mathrm{P}} \quad \mathrm{Z}_{1\mathrm{P}}]^{\mathrm{T}}$ in the D-CS of the whole teeth and the coordinate $[\mathrm{X}_{2\mathrm{P}} \quad \mathrm{Y}_{2\mathrm{P}} \quad \mathrm{Z}_{2\mathrm{P}}]^{\mathrm{T}}$ in the D-CS of a single tooth.

$$\begin{bmatrix} \mathrm{X}_{1\mathrm{P}} \\ \mathrm{Y}_{1\mathrm{P}} \\ \mathrm{Z}_{1\mathrm{P}} \end{bmatrix} = \begin{bmatrix} \left(1-\frac{\mathrm{Z}_{\mathrm{D}'}}{|\mathrm{Z}_{\mathrm{D}'}|}\right)\mathrm{X}_{\mathrm{Z}}{}^2+\mathrm{Z}_{\mathrm{D}'} & \left(1-\frac{\mathrm{Z}_{\mathrm{D}'}}{|\mathrm{Z}_{\mathrm{D}'}|}\right)\mathrm{X}_{\mathrm{Z}}\mathrm{Y}_{\mathrm{Z}}-\mathrm{Z}_{\mathrm{Z}}\sin\theta & \left(1-\frac{\mathrm{Z}_{\mathrm{D}'}}{|\mathrm{Z}_{\mathrm{D}'}|}\right)\mathrm{X}_{\mathrm{Z}}\mathrm{Z}_{\mathrm{Z}}+\mathrm{Y}_{\mathrm{Z}}\sin\theta & \mathrm{X}_{\mathrm{O_D}'} \\ \left(1-\frac{\mathrm{Z}_{\mathrm{D}'}}{|\mathrm{Z}_{\mathrm{D}'}|}\right)\mathrm{X}_{\mathrm{Z}}\mathrm{Y}_{\mathrm{Z}}+\mathrm{Z}_{\mathrm{Z}}\sin\theta & \left(1-\frac{\mathrm{Z}_{\mathrm{D}'}}{|\mathrm{Z}_{\mathrm{D}'}|}\right)\mathrm{Y}_{\mathrm{Z}}{}^2+\mathrm{Z}_{\mathrm{D}'} & \left(1-\frac{\mathrm{Z}_{\mathrm{D}'}}{|\mathrm{Z}_{\mathrm{D}'}|}\right)\mathrm{Y}_{\mathrm{Z}}\mathrm{Z}_{\mathrm{Z}}-\mathrm{X}_{\mathrm{Z}}\sin\theta & \mathrm{Y}_{\mathrm{O_D}'} \\ \left(1-\frac{\mathrm{Z}_{\mathrm{D}'}}{|\mathrm{Z}_{\mathrm{D}'}|}\right)\mathrm{X}_{\mathrm{Z}}\mathrm{Z}_{\mathrm{Z}}-\mathrm{Y}_{\mathrm{Z}}\sin\theta & \left(1-\frac{\mathrm{Z}_{\mathrm{D}'}}{|\mathrm{Z}_{\mathrm{D}'}|}\right)\mathrm{Y}_{\mathrm{Z}}\mathrm{Z}_{\mathrm{Z}}+\mathrm{X}_{\mathrm{Z}}\sin\theta & \left(1-\frac{\mathrm{Z}_{\mathrm{D}'}}{|\mathrm{Z}_{\mathrm{D}'}|}\right)\mathrm{Z}_{\mathrm{Z}}{}^2+\mathrm{Z}_{\mathrm{D}'} & \mathrm{Z}_{\mathrm{O_D}'} \end{bmatrix} \begin{bmatrix} \mathrm{X}_{2\mathrm{P}} \\ \mathrm{Y}_{2\mathrm{P}} \\ \mathrm{Z}_{2\mathrm{P}} \\ 1 \end{bmatrix} (12)$$

The rotation axis and angle can get in a similar way. Additionally, the translation vector of the origin of the A-CS in the whole teeth and the R-CS in a single tooth is $\boldsymbol{T}_{\boldsymbol{O_AO_R}} = [\mathrm{X}_{\mathrm{R}}-\mathrm{X}_{\mathrm{A}} \quad \mathrm{Y}_{\mathrm{R}}-\mathrm{Y}_{\mathrm{A}} \quad \mathrm{Z}_{\mathrm{R}}-\mathrm{Z}_{\mathrm{A}}]^{\mathrm{T}}$. Substitute these values into Equation $(11, 12)$ to get the transformation relationship between the A-CS of the whole teeth and the R-CS of the single tooth.

3.5 Example of Multi-stage Operation of Teeth Model in the Coordinate Systems of A-CS and R-CS

Long-term digital tooth operations and movements applied in medicine like orthodontics occur as a result of mechanical and biologic processes [32]. It divides rotations at a large angle and long distances in many stages to facilitate tooth adaptation and recovery. The angle at each stage was often less than 1.5 degrees in practice and the movement distance was less than 0.2 mm in each stage. We chose the digital teeth model of the lower jaw with the A-CS of the whole teeth and the R-CS of every single tooth in multiple stages. Though the Incisors, canines and molars have different morphologies, the method of the coordinate system establishment is well suitable in all teeth. And it provides the automatic way to establish the R-CS for every tooth. Then we operate the digital model to realize the visualization of the orthodontic process. Figure 5 shows the four different stages in the operations by using the two different coordinate systems. The result shows that the coordinate systems of A-CS and R-CS are convenient to easily calculate the relationships based on rotations and translations, as well as operate the digital model independently. The digital teeth models operated in the software are finally used to manufacture by 3D printing as templates to produce transparent braces.

ISSN: 2414-1895 DOI: 10.6919/ICJE.202208_8(8).0050

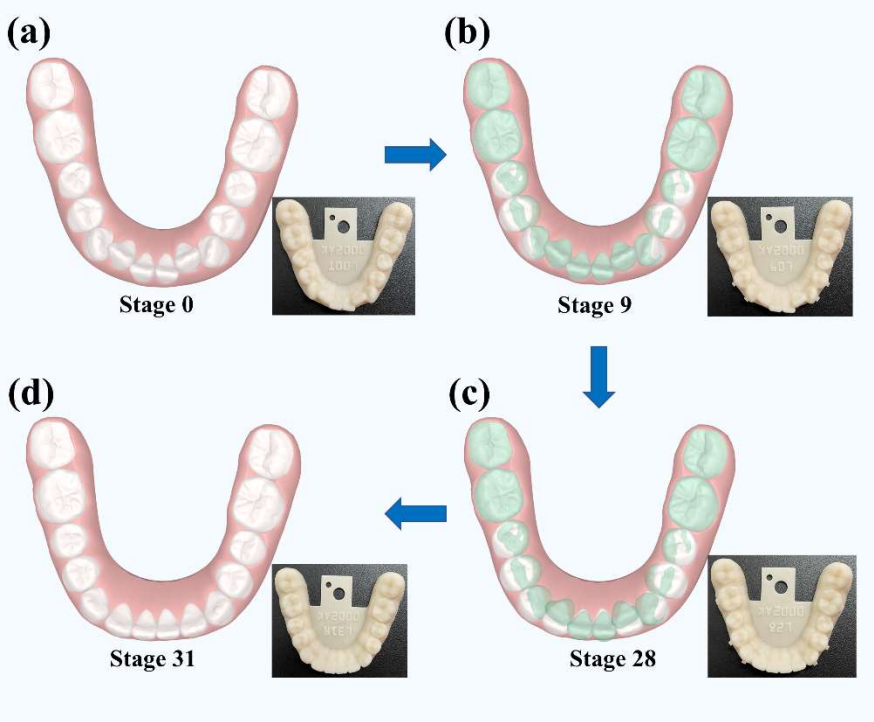

Figure 5. The digital models in orthodontic virtual treatment and 3D printing physical models in four stages of teeth operations, which are based on rotations and translations correspondingly. The green part indicates the initial dental model and the white part shows the condition of the teeth model after the operation in the stage. The stages contain (a) the initial teeth model, (b) stage nine, (c) stage 28 and (d) stage 31.

4. Conclusion

In this work, the method of selecting three available feature points in the whole teeth to calculate the three coordinate axes by vector product and the midpoint is easy to implement and universal to various teeth models. The A-CS, established by three positive directions axes based on the practical operation rule and the midpoint, is the reference system to judge the situation of every single tooth and decides the multiple views facing different axes to observe the model. For a single tooth, the coordinate changes when it rotates and translates in the A-CS, while the relative position of each point is unchanged relative to the tooth itself. To solve the problem, the R-CS of every single tooth is established by the three automatically generated axes with the method of OBB based on the PCA and the midpoint of all points on the digital triangle mesh. The R-CS makes every single tooth independently operate and analyze into reality, and avoids the interferences of other parts of the model. It is R-CS that solves the problem successfully. The combination of the A-CS and R-CS provides a feasible way to operate the part of a model independently and judge its situation in an unchanged coordinate system. The axes of two types of coordinate systems are used to calculate the mutual transformation, which realizes the unification of different coordinate systems. A transformation matrix of three rows and four columns implements rotation and translation simultaneously in different coordinates or coordinate systems. It replaces the traditional calculation way that a matrix control rotation and a vector control translation, which provides a more intuitive way to characterize the single-stage operation. One operation corresponded to a conversion matrix using this matrix to calculate tooth operations is of great significance for multiple and staged model operations. According to the characteristics of the Cartesian coordinate system, it is convenient that the rotation matrix is calculated by the axis-angle method when the initial and final coordinates or one of the coordinate axes has been known. The detailed calculation of digital teeth models is given to calibrate and quantify operations in a more appropriate way. Potential applications of the detailed calculations

ISSN: 2414-1895 DOI: 10.6919/ICJE.202208_8(8).0050

include multiple stages digital teeth models operations and the design of software of more intuitive calibration and quantitative operations.

Acknowledgments

The research thanks Zhihao Ma for their assistance in acquiring and operating the 3D dental models, and Kunming Wei for discussing the key concepts of the manuscript.

Funding: This research was funded by Key-Area Research and Development Program of Guangdong Province (2020B090924001) and Guangzhou Science and Technology planning project (202002030210, 202102021302).

References

[1] S. Listl, J. Galloway, P.A. Mossey, W. Marcenes, Global Economic Impact of Dental Diseases, J Dent Res 94(10) (2015) 1355-61, https://doi.org/10.1177/0022034515602879.

[2] J.E. Frencken, P. Sharma, L. Stenhouse, D. Green, D. Laverty, T. Dietrich, Global epidemiology of dental caries and severe periodontitis - a comprehensive review, J Clin Periodontol 44 Suppl 18 (2017) S94-S105, https://doi.org/10.1111/jcpe.12677.

[3] M.A. Peres, L.M.D. Macpherson, R.J. Weyant, B. Daly, R. Venturelli, M.R. Mathur, S. Listl, R.K. Celeste, C.C. Guarnizo-Herreño, C. Kearns, H. Benzian, P. Allison, R.G. Watt, Oral diseases: a global public health challenge, The Lancet 394(10194) (2019) 249-260, https://doi.org/10.1016/s0140-6736(19)31146-8.

[4] L. McNamara, J.A. McNamara, Jr., M.B. Ackerman, T. Baccetti, Hard- and soft-tissue contributions to the esthetics of the posed smile in growing patients seeking orthodontic treatment, Am J Orthod Dentofacial Orthop 133(4) (2008) 491-9, https://doi.org/10.1016/j.ajodo.2006.05.042.

[5] M.S. Alhammadi, E. Halboub, A.A. Al-Mashraqi, M. Al-Homoud, S. Wafi, A. Zakari, W. Mashali, Perception of facial, dental, and smile esthetics by dental students, J Esthet Restor Dent 30(5) (2018) 415-426, https://doi.org/10.1111/jerd.12405.

[6] M.K. Afshar, A. Eskandarizadeh, M. Torabi, M.J. Mousavi, I. Mohammadzadeh, Patient Satisfaction with Dental Appearance and Related FactorsA Cross Sectional Study, Journal of Evolution of Medical and Dental Sciences 8(48) (2019) 3569-3574, http://dx.doi.org/10.14260/jemds/2019/771.

[7] N. Gul Amuk, E. Karsli, G. Kurt, Comparison of dental measurements between conventional plaster models, digital models obtained by impression scanning and plaster model scanning, Int Orthod 17(1) (2019) 151-158, https://doi.org/10.1016/j.ortho.2019.01.014.

[8] S.-H. Kang, Y.-H. Kim, M.-K. Kim, Comparison of digital dental images yielded by digital dental casts, cone-beam computed tomography, and multislice computed tomography for measurement of dental area, Oral Radiology 33(1) (2016) 23-31, http://dx.doi.org/10.1007/s11282-016-0242-z.

[9] M. Kašparová, S. Halamová, T. Dostálová, A. Procházka, Intra-Oral 3D Scanning for the Digital Evaluation of Dental Arch Parameters, Applied Sciences 8(10) (2018), http://dx.doi.org/10.3390/app8101838.

[10] M. Ioshida, B.A. Munoz, H. Rios, L. Cevidanes, J.F. Aristizabal, D. Rey, H. Kim-Berman, M. Yatabe, E. Benavides, M.A. Alvarez, S. Volk, A.C. Ruellas, Accuracy and reliability of mandibular digital model registration with use of the mucogingival junction as the reference, Oral Surg Oral Med Oral Pathol Oral Radiol 127(4) (2019) 351-360, http://dx.doi.org/10.1016/j.oooo.2018.10.003.

[11] S. Akyalcin, B.E. Cozad, J.D. English, C.D. Colville, S. Laman, Diagnostic accuracy of impression-free digital models, Am J Orthod Dentofacial Orthop 144(6) (2013) 916-22, https://doi.org/10.1016/j.ajodo.2013.04.024.

[12] S.Y. Kang, J.M. Yu, J.S. Lee, K.S. Park, S.Y. Lee, Accuracy Analysis of Digital Dental Model Data acquired by Dental Cone Beam Computed Tomography, Journal of Magnetics 25(4) (2020) 663-669, https://doi.org/10.4283/jmag.2020.25.4.663.

[13] F. Mangano, A. Gandolfi, G. Luongo, S. Logozzo, Intraoral scanners in dentistry: a review of the current literature, BMC Oral Health 17(1) (2017) 149, https://bmcoralhealth.biomedcentral.com/ articles/10.1186/s12903-017-0442-x.

ISSN: 2414-1895 DOI: 10.6919/ICJE.202208_8(8).0050

[14] S. Logozzo, E.M. Zanetti, G. Franceschini, A. Kilpelä, A. Mäkynen, Recent advances in dental optics–Part I: 3D intraoral scanners for restorative dentistry, Optics and Lasers in Engineering 54 (2014) 203-221, http://dx.doi.org/10.1016/j.optlaseng.2013.07.017.

[15] M. Imburgia, S. Logozzo, U. Hauschild, G. Veronesi, C. Mangano, F.G. Mangano, Accuracy of four intraoral scanners in oral implantology: a comparative in vitro study, BMC Oral Health 17(1) (2017) 92, https://doi.org/10.1186/s12903-017-0383-4.

[16] T. Wu, E.H.M. Cheung, Enhanced STL, The International Journal of Advanced Manufacturing Technology 29(11-12) (2005) 1143-1150, http://dx.doi.org/10.1007/s00170-005-0001-5.

[17] M. Szilvasi-Nagy, G. Matyasi, Analysis of STL files, Mathematical and Computer Modelling 38(7-9) (2003) 945-960, http://dx.doi.org/10.1016/S0895-7177(03)90079-3.

[18] S. Khanna, D. Rao, S. Panwar, B.A. Pawar, S. Ameen, 3D Printed Band and Loop Space Maintainer: A Digital Game Changer in Preventive Orthodontics, Journal of Clinical Pediatric Dentistry 45(3) (2021) 147-151, https://doi.org/10.17796/1053-4625-45.3.1.

[19] M. Santoro, S. Galkin, M. Teredesai, O.F. Nicolay, T.J. Cangialosi, Comparison of measurements made on digital and plaster models, American journal of orthodontics and dentofacial orthopedics 124(1) (2003) 101-105, https://doi.org/10.1016/s0889-5406(03)00152-5.

[20] L.T. Camardella, E.K.C. Rothier, O.V. Vilella, E.M. Ongkosuwito, K.H. Breuning, Virtual setup: application in orthodontic practice, Journal of Orofacial Orthopedics/Fortschritte der Kieferorthopädie 77(6) (2016) 409-419, https://doi.org/10.1007/s00056-016-0048-y.

[21] D. Claus, J. Radeke, M. Zint, A.B. Vogel, Y. Satravaha, F. Kilic, R. Hibst, B.G. Lapatki, Generation of 3D digital models of the dental arches using optical scanning techniques, Seminars in Orthodontics 24(4) (2018) 416-429, https://doi.org/10.1053/j.sodo.2018.10.006.

[22] K. Hayashi, R. DeLong, I. Mizoguchi, Comparison of the finite helical axis and the rectangular coordinate system in representing orthodontic tooth movement, J Biomech 39(16) (2006) 2925-33, https://doi.org/10.1016/j.jbiomech.2005.10.030.

[23] S.F. Lu, X.M. Lin, X. Han, Virtual-real Registration of Augmented Reality Technology Used in the Cerebral Surgery Lesion Localization, Fifth International Conference on Instrumentation & Measurement, Computer, Communication, and Control (IMCCC), Qinhuangdao, PEOPLES R CHINA, 2015, pp. 619-624, https://doi.org/10.1109/IMCCC.2015.136.

[24] M.L. Wu, J.C. Chien, C.T. Wu, J.D. Lee, An Augmented Reality System Using Improved-Iterative Closest Point Algorithm for On-Patient Medical Image Visualization, Sensors (Basel) 18(8) (2018), https://doi.org/10.3390/s18082505.

[25] I.T. Jolliffe, J. Cadima, Principal component analysis: a review and recent developments, Philos Trans A Math Phys Eng Sci 374(2065) (2016) 20150202, https://doi.org/10.1098/rsta.2015.0202.

[26] Q. Chen, X. Jin, H. Zhu, H.S. Salehi, K. Wei, 3D distribution of dental plaque on occlusal surface using 2D-fluorescence-image to 3D-surface registration, Comput Biol Med 123 (2020) 103860, https://doi.org/10.1016/j.compbiomed.2020.103860.

[27] J. Hyttinen, P. Falt, H. Jasberg, A. Kullaa, M. Hauta-Kasari, Computational Filters for Dental and Oral Lesion Visualization in Spectral Images, IEEE Access 9 (2021) 145148-145160, https://doi.org/10.1109/ACCESS.2021.3121815.

[28] S. Gottschalk, M.C. Lin, D. Manocha, OBBTree: a hierarchical structure for rapid interference detection, Proceedings of the 23rd annual conference on Computer graphics and interactive techniques (1996), http://dx.doi.org/10.1145/237170.237244.

[29] A. Iones, S. Zhukov, A. Krupkin, On optimality of OBBs for visibility tests for frustum culling, ray shooting and collision detection, Proceedings. Computer Graphics International (Cat. No.98EX149) (1998) 256-263, https://doi.org/10.1109/CGI.1998.694275.

[30] J.-W. Chang, W. Wang, M.-S. Kim, Efficient collision detection using a dual OBB-sphere bounding volume hierarchy, Computer-Aided Design 42(1) (2010) 50-57, http://dx.doi.org/10.1016/j.cad.2009. 04. 010.

[31] S. Keiser-Nielsen, Digitalization of dental recording, Forensic science international 20(2) (1982) 153-161, https://doi.org/10.1016/0379-0738(82)90140-2.

ISSN: 2414-1895 DOI: 10.6919/ICJE.202208_8(8).0050

[32] R. Hamanaka, S. Yamaoka, T.N. Anh, J.Y. Tominaga, Y. Koga, N. Yoshida, Numeric simulation model for long-term orthodontic tooth movement with contact boundary conditions using the finite element method, Am J Orthod Dentofacial Orthop 152(5) (2017) 601-612, https://doi.org/10.1016/j.ajodo.2017.03.021.